International Journal of Biological, Physical and Chemical Studies
ISSN: 2709-1554
DOI: 10.32996/ijbpcs
Journal Homepage: www.al-kindipublisher.com/index.php/ijbpcs

IJBPCS
AL-KINDI CENTER FOR RESEARCH AND DEVELOPMENT

| REVIEW ARTICLE

Experimental Performance Enhancement of a Standing-Wave Thermoacoustic Cooler Using a Random Stainless-Steel Stack and a Water-Cooled Auxiliary Heat Exchanger

Sanchay Kanti Barua[1]* and Kaberi Das[2]
[1,2] Independent Researcher, Mastermind International School, Chattogram, Bangladesh*
ORCID: 0009-0005-7025-7172 (Sanchay Kanti Barua)
ORCID: 0009-0008-1617-612X (Kaberi Das)
Corresponding Author: Sanchay Kanti Barua, **E-mail**: sanchaykantibarua@gmail.com

| ABSTRACT
Traditional vapor compression refrigeration systems are highly dependent on synthetic refrigerants, which are harmful to the ozone layer and contribute to global warming. Thermoacoustic cooling is an emerging alternative that uses high-amplitude acoustic waves to create refrigeration without moving parts or chemical refrigerants. In this study, we experimentally examined the performance of a standing-wave thermoacoustic cooler driven by a loudspeaker with a randomly oriented stainless-steel mesh stack and the effect of a water-cooled auxiliary heat exchanger on the system performance. A cylindrical PVC resonating chamber was connected to a loudspeaker and an amplifier. The frequency of operation was varied from 50 Hz to 200 Hz to determine the resonant conditions. Four different stack heights of 18-mesh stainless steel (4, 5, 6, and 7 cm) were tested. Calibrated LM35 sensors were used to measure the temperatures at both the hot and cold reservoirs. A copper-coiled auxiliary heat exchanger was attached to a closed water-circulation loop at the hot end to remove the collected heat. An optimum resonance frequency of 113 Hz was determined. The largest temperature difference (19.4°C) between the hot and cold sides was obtained with a 6-cm stack height. The cold-side temperature drop was further increased by 4.1°C upon activation of the auxiliary heat exchanger, and the heat saturation time of the cold side was reduced. This random stainless-steel mesh stack geometry not only exhibits a competitive heat transfer performance but also offers practical fabrication benefits. To realize thermoacoustic cooling in the steady state, active heat rejection through a water-cooled auxiliary exchanger is necessary, and the cooling span and steady-state cold temperature are significantly enhanced.

| KEYWORDS
Thermoacoustic cooling; Standing-wave resonator; Random mesh stack; Auxiliary heat exchanger; Sustainable refrigeration; Stainless-steel stack; Resonance frequency optimization

| ARTICLE INFORMATION
ACCEPTED: 01 May 2026 **PUBLISHED:** 06 June 2026 **DOI:** 10.32996/ijbpcs.2026.8.2.1

Introduction

1.1 Background and Motivation

The global cooling technology market is growing rapidly owing to climate change, global warming, urbanization, industrialization, thermal comfort, and food preservation. Vapor-compression refrigeration systems are commonly employed in domestic, commercial, and industrial applications worldwide. However, the common refrigerants in these systems—CFCs, HCFCs, and HFCs—have high global warming potential (GWP), high ozone depletion potential (ODP), and are classified as greenhouse gases (GHGs). International environmental protocols, such as the Montreal Protocol and Kigali Amendment, have set timelines for phasing out harmful refrigerants; nevertheless, conventional refrigeration systems still face significant hurdles in achieving long-term sustainability [1].

In response to these concerns, many researchers have focused on developing environmentally friendly and energy-efficient

cooling technologies. The potential of thermoacoustic refrigeration (TAR) to be a non-harmful refrigeration technology with limited moving mechanical components makes it a promising alternative to cooling with refrigerants and compressors. Acoustic energy is used to produce a temperature difference in a resonator containing a working gas, which is the basis of TAR. Acoustic waves generated by a loudspeaker or acoustic driver provide periodic compression and expansion of the gas molecules in the resonator tube of a standing wave thermoacoustic refrigerator. When a porous medium (stack) is inserted in the correct position within the sound field, a refrigeration effect occurs between the cold and hot heat exchangers because heat is transferred between the oscillating gas parcels and the surface of the stack [2].

Thermoacoustic refrigeration is advantageous because it does not use refrigerants, compressors, or lubricants that can negatively affect the environment. Instead, the working fluid can be a nontoxic gas, such as air, helium, or a helium/argon mixture. Thermoacoustic refrigeration has proven to be a promising field of research in sustainable cooling and renewable energy systems owing to its simple design, low maintenance requirements, high operational reliability, and environmentally friendly operation.

These implications are more relevant to developing nations such as Bangladesh, where the demand for cooling is growing at a higher rate because of rising ambient temperatures, population, and urbanization. Owing to the widespread installation of conventional air-conditioning systems, electricity consumption has been significant in providing cooling requirements, and there are concerns about refrigerant leakage and greenhouse gas emissions. Hence, there is a growing demand for the development of local and environmentally friendly cooling technologies. Thermoacoustic cooling systems are environmentally friendly, easy to build and operate, and can utilize renewable or waste energy sources [3].

Most previous research on thermoacoustic refrigeration has focused on standing-wave-type refrigerators using parallel-plate stacks in cylindrical resonators. The operating frequency, position of the stack, shape of the resonator, distance between the stack and resonator, composition of the working gas, acoustic amplitude, and size of the resonator have been studied as key parameters that affect the thermoacoustic behavior. It has been shown that these parameters can have a significant effect on the achievable temperature difference, COP, and cooling power of the thermoacoustic refrigerator. Most earlier studies have focused on regular parallel-stack configurations; however, few studies have investigated randomly packed porous stack configurations or the integration of auxiliary heat exchangers.

In recent years (2018–2025), there has been a trend of creating alternative stack designs, such as wire mesh, spiral mesh, porous ceramic stacks, and stainless-steel regenerators, to enhance the thermal interaction between oscillating gas and stack materials. The porous and mesh structures of stacks have been reported to exhibit better heat transfer performance and sound interaction owing to their large surface area and turbulence. Furthermore, it has been found that the inclusion of additional heat exchangers can enhance the thermal stability and heat rejection capacity of thermoacoustic systems [4].

Although significant progress has been made, there has been limited research on the thermoacoustic efficiency of other configurations of random stainless-steel mesh stacks with an additional hot heat exchanger in resonator tubes. In particular, research on random porous stack structure configurations for low-frequency SW operations using air drives is lacking. Therefore, further research is required to understand the thermoacoustic cooling performances of various auxiliary heat exchange mechanisms and random-stack geometries.

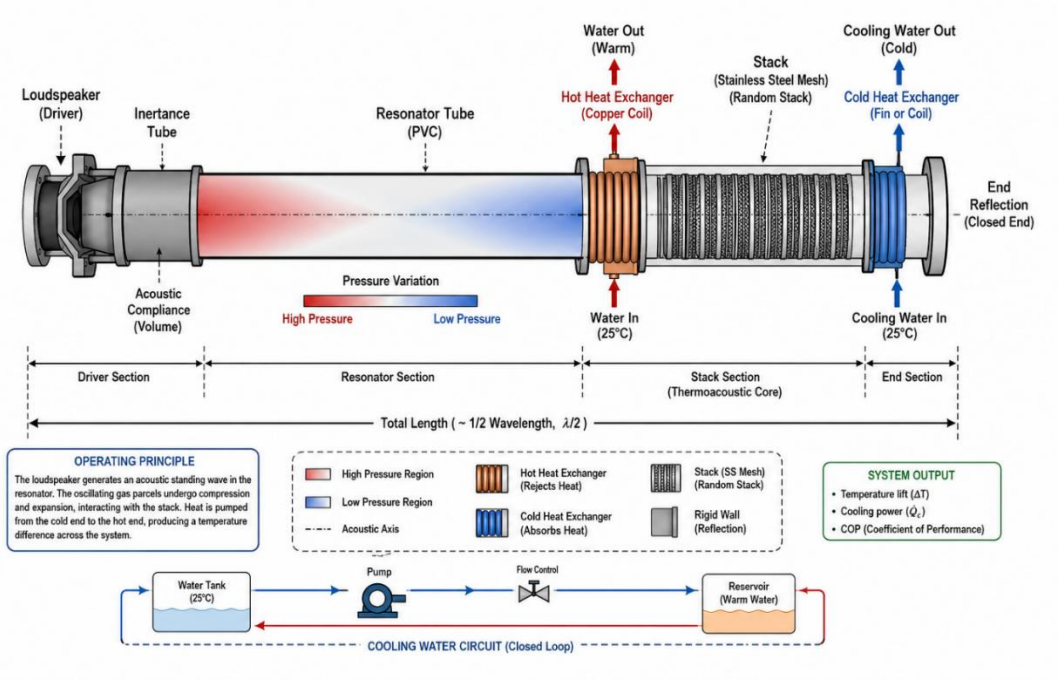

Figure 1. *Schematic overview of a basic standing-wave thermoacoustic cooling system*

In this study, the existing shortcomings were overcome by designing a standing wave thermoacoustic cooling system in which a random 3D porous stack of stainless steel was used, in addition to an extra water-cooled hot heat exchanger in the resonator tube. This study analyzed the effect of the operating frequency on the temperature difference generated by the system and its improvement in the performance of the SWTACS using a random porous stack geometry and better heat exchange mechanisms.

The present study aimed to:

- Design and development of a thermoacoustic cooling system based on a randomly arranged porous stainless-steel stack
- To improve the thermal performance of the system by adding another hot heat exchanger to the resonator tube
- To compare the cooling performance of a TA refrigerator with different operating frequencies, random stack geometry, and artificial heat exchange
- To contribute to the development of environmentally friendly and sustainable cooling technologies in Bangladesh and other developing countries

The outcomes of this study are expected to provide valuable information for developing optimal designs for thermoacoustic refrigeration systems and gain further insights into global efforts to promote sustainable and environmentally friendly cooling technologies [5].

1.2 Related Work

In Ref. In [6], the authors presented the performance of optimizing a traveling-wave system with a stack configuration thermoacoustic refrigerator to maximize the coefficient of performance and cooling power output. Linear thermoacoustic theory was used to optimize the geometry of the stack heat exchanger and resonator. The working gases used were helium and air, which have the same thermophysical properties and are economically feasible. An ordinary loudspeaker with a gas spring at the back was used as the acoustic driver. The optimized system generated a temperature difference of 28 K between the top and bottom of the stack. The cooling powers were forecasted as 349 W at COP 0.998 with helium and 139 W at COP 1.133 with air. The DELTAEC program was used to obtain several simulation results that were consistent with the theoretical results [6].

For clarity and ease of analysis, the authors used the linear thermoacoustic theory of Rott to obtain normalized expressions for cooling and acoustic power for the most important design parameters, defined by an input power of 500 W and a thermal gradient between the heat reservoirs of 28 K. The ratio of the heat capacity of the stack material to its thermal conductivity was normalized. The effects of gas spacing (thermal penetration depth at 85% proportion) and resonance frequency on the system were examined. The theoretical COP values for air were 1.72 at 300 Hz and 1.53 at 400 Hz, whereas the ΔEC predicted COP values were lower owing to unexpected practical losses: 347 W, COP = 1.02 for helium, and 224 W,

COP = 0.79 for air, as predicted by the simulation. To understand the impact of non-ideal phenomena on system performance and to verify the approach for modelling, the theoretical and simulated results were compared [7].

The design and performance of a thermoacoustic cooler using CO2 as the working fluid are discussed herein. The system can be further developed into a helium-based thermoacoustic cooler with a constant operating frequency of 500 Hz. A dual heat exchanger and half-wavelength resonator were designed to maximize the overall net cooling capacity of the system. The results of this study comprise a set of DeltaEC simulations using various setups and stack configurations. The results demonstrated that the operation of the two heat exchangers in the dual-stack configuration was better than that in the single-stack configuration, and demonstrated the viability of this configuration in designing cooling systems [8].

This study focuses on an experimental investigation of travelling-wave thermoacoustic refrigeration (TWR) instead of a theoretical investigation of stack configuration thermoacoustic refrigerators (TOR), as explained by Prashantha et al. Using two moving-coil loudspeakers in a resonator as the source of temperature control, this study presents an experimental verification of the possibility of precisely controlling the temperature of an elemental ceramic thermoacoustic stack. An experimental apparatus was designed, and DeltaEC was used to analyze the system response to the dynamic boundary conditions for the two system setups: a dual-speaker system and a ceramic stack system. The relative phase difference between the two drivers can be controlled to vary the temperature, and even the relative phase difference can be reversed in 'real time' to provide a traveling-wave effect. The results suggest that the efficiency of refrigeration can be finely controlled according to wave phenomena, which achieves greater control of thermoacoustic temperature control in precision and extreme applications [9].

This study explores the design of a standing wave thermoacoustic refrigerator with a standard loudspeaker and uses numerical simulation DELTAEC to realize a low-cost design. The main design parameters that influence the refrigeration power and performance of the system were determined and subsequently optimized. The optimized design satisfied the required refrigeration output of 25 K, with a coefficient of performance (COP) of 1.956 and an overall efficiency of 113.43%. Based on the results presented, DELTAEC is a potential, suitable, efficient, and cost-effective tool for designing an SWT refrigeration system [10].

This study is not a continuation of the study on thermoacoustic refrigerators with stacks performed by Prashantha et al. (2022); instead, it is a theoretical study of a standing-wave thermoacoustic refrigerator (SW-TAR) driven by a loudspeaker under various boundary conditions. Based on linear thermoacoustic theory, a simple model was constructed, and a parametric study was conducted to examine how the end impedance of the resonating tube affects the performance of the system in terms of acoustic characteristics and refrigeration effect. The difference in end impedance (which depends on the boundary conditions) significantly influences the refrigeration effect; therefore, it is important to determine the optimum frequency of the driving. The following work provides useful information and design parameters to customize TAR designs for various applications [11].

Although the theoretical aspects of stack-type thermoacoustic refrigerators were not evaluated in this study, the effect of the spiral rubber stack on the cooling capacity of a thermoacoustic refrigeration system comprising a stack (acrylic resonance tube) and air as the working gas was investigated. It was found that the temperature on the hot side increased and that on the cold side decreased over time, which increased the temperature difference across the sides of the stack [12].

In this study, SW models of a thermoacoustic refrigerator system with various thermoacoustic stack materials were considered to investigate their effects on the system performance. The results demonstrate that the performance of the thermoacoustic system is significantly influenced by the stack material; therefore, the use of thermoacoustics in environmentally friendly applications, such as refrigeration and power generation, is becoming significant [13]. A systematic study on the effect of auxiliary heat rejection at the hot end of the stack is lacking in the experimental literature. During a test run, in most laboratory setups, the hot-side temperature can increase freely, resulting in progressive thermal saturation; the higher the hot-end temperature, the lower the refrigeration potential and poorer the steady-state performance. Table 1 summarizes the important parameters of the selected studies [13].

Table 1. *Summary of key prior thermoacoustic cooling studies and their operating parameters*

Authors (Year)	Stack / Regenerator Type	Working Gas	Operating Frequency (Hz)	Maximum ΔT (°C)	Auxiliary HX	Major Contribution
Jakub Kajurek & Artur Rusowicz (2018)	Parallel plate stack	Air	200–300	~15	No	Demonstrates that the resonator length and operating frequency significantly affect the thermoacoustic cooling performance. (AGRIS)
M. A. Alamir & A. A. Elamer (2019)	Standing-wave stack	Helium / Air	100–400	~20	No	Used deltaEC optimization to balance the COP and temperature difference in standing-wave thermoacoustic refrigerators (bura.brunel.ac.uk)
X. Mao et al. (2020)	Stainless-steel wire mesh	Air	100–180	16–17	Partial	Improved heat transfer and thermo–viscous interaction using metallic wire-mesh regenerators
Zahra Bouramdane et al. (2022)	Corrugated parallel plates	Air	~150	~18	No	: Numerical CFD study showing that geometric plate modification affects ΔT and acoustic efficiency. (Springer)
B. G. Prashantha et al. (2022)	Stack–HX optimized structure	Helium / Air	200–400	28	Integrated HX optimization	Theoretical optimization of stack and heat exchanger configurations for improved COP and cooling power (Springer)
B. G. Prashantha et al. (2023)	Parallel stack with optimized spacing	Air / Helium	200–400	28	Yes	Effects of resonance frequency and gas spacing on the performance of a thermoacoustic refrigerator (Springer)
Luca Perna et al. (2023)	Wire mesh regenerator	Air	100–300	~18	Partial	Developed a thermo–viscous transport model for wire-mesh stacks and experimentally validated its efficiency behavior. (ScienceDirect)
Rina Sa Anugrah et al. (2024)	High-porosity wire mesh (#18)	Air	~100	4.8 temperature reduction	Yes	Showed that a larger-porosity wire mesh improves cooling effectiveness and thermal performance. (semarakilmu.com.my)
Present Study (2026)	Random stainless-steel mesh regenerator	Air	50–200	19.4	Yes (water-cooled HX)	Improved thermal stability and enhanced cooling effectiveness were achieved using a random SS mesh with an auxiliary water-cooled heat exchanger.

1.3 Research Gap and Novelty

Two points in the current literature have not been sufficiently discussed: (1) little research is available on the application of thermoacoustic cooling to a vehicle's HVAC system, and (2) there is insufficient research on the optimization of the system. First, there has been no research on how the performance of randomly oriented stacks of meshes changes as a system with changes in frequency and length; therefore, it has not been sufficiently studied to provide guidance in practice. Random meshes can readily be fabricated from commercially available wire cloth, are inexpensive, but are known to provide turbulent, nonlinear thermoacoustic theory, and there are no performance maps. Second, the quantitative performance to date of active heat rejection compared to passive natural convection has not been carefully investigated using a controlled single-effect test.

The gaps in the existing knowledge are addressed in this study by (i) an experimental parametric study in an air atmosphere with an 18-mesh stainless-steel random stack at different acoustic frequencies and stack lengths, and (ii) a comparative study of the system performance of the hot end with and without the help of a water-cooled auxiliary copper-coil heat exchanger with other parameters fixed. The results will be valuable for the design of low-cost prototype thermoacoustic coolers and will provide a reference for comparison with the behavior of future computational studies on random media stacks [14].

2. Theoretical Background

Thermoacoustic refrigeration is based on the correlation between acoustic pressure and entropy oscillations in a compressible gas. In a closed–open resonator tube, the gas is compressed (pressure maximum) and rarefied (pressure minimum) at any cross-section of the tube alternately with time. If the gas parcel is moved towards the pressure antinode, it is compressed and heated; if it is moved towards the pressure node, it is expanded and cooled.

The gas parcel in the middle of a pore in a porous stack will experience both oscillatory displacement and temperature change if the porous stack is oriented such that it spans a portion of the displacement antinode to the pure displacement antinode (maximum velocity, minimum pressure) and the temperature antinode to the pressure antinode (maximum pressure, minimum velocity). The volumetric heat capacity of the solid walls of the stack is considerably higher than that of the working gas and can be regarded as local thermal reservoirs. During the half cycle in which the parcel moves towards the hot end, it deposits heat to the stack wall at a marginally cooler temperature than the wall, and during the half cycle when it returns to the stack wall, it absorbs heat from the wall at a marginally warmer temperature than the wall.

This asymmetric heat exchange is known as the Wheatley streaming mechanism and assists in transferring a net amount of thermal energy to the hot end of the stack over a cycle. The heat pumping rate is determined by the amplitude of the acoustic displacement, acoustic pressure amplitude, thermophysical properties of the gas/stack material, geometry of the stack pores, and the location of the stack in the standing wave. To achieve optimal performance, the temperature gradient (dT/dx) of the stack must be close to the critical temperature gradient, which is defined as

$$\nabla T_{crit} = T_m \cdot U_1 \cdot \beta / (A \cdot T_p \cdot c_p \cdot k)$$

Here, T_m is the mean temperature, U_1 is the amplitude of the volumetric velocity of the sound wave, β is the thermal expansion coefficient, A is the cross-sectional area, T_p is the acoustic period, c_p is the specific heat at constant pressure, and k is the thermal conductivity of the working gas. When the applied temperature difference is less than ∇T_{crit}, the applied cooling process of the stack is the opposite of that of the refrigerator (cold to hot). If the gradient exceeds ∇T_{crit}, it acts as a heat engine or prime mover.

The COP of a thermoacoustic refrigerator is defined in a manner similar to that of a vapor-compression refrigerator, as COP = Qc/Wa, where Qc is the rate at which heat is extracted at the cold heat exchanger, and Wa is the acoustic power used. The COP values of air-based standing wave coolers typically range between 0.1 and 0.5. These values are significantly smaller than the Carnot value but comparable to those of other new refrigeration technologies with the same cooling power [15].

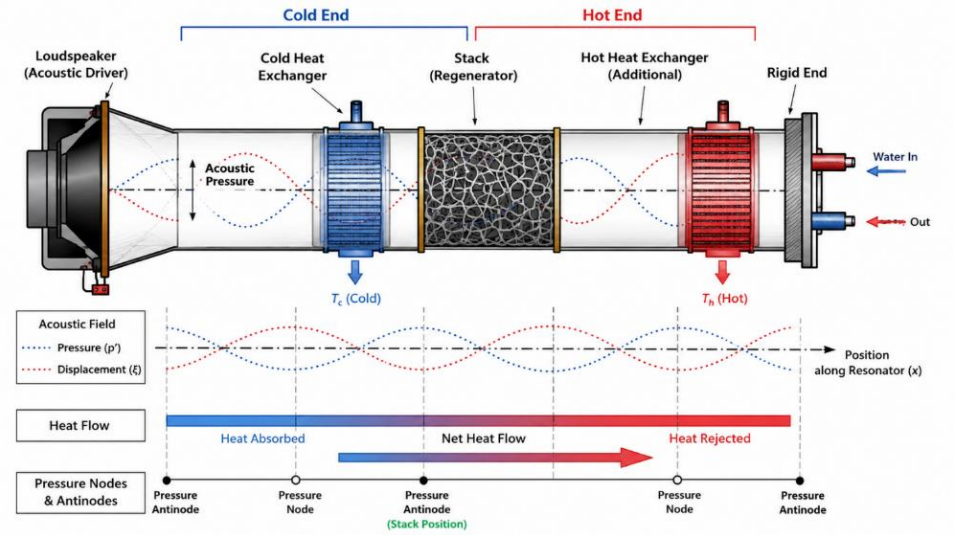

Figure 2. *Schematic cross-section of the standing-wave thermoacoustic cooler illustrating acoustic wave structure*

3. Methodology

3.1 Experimental Setup

The experiment was performed using a 50 mm diameter and 1500 mm long complete PVC resonator tube. PVC was chosen for its low thermal conductivity (0.19W/m·K) to lower unwanted heat conduction in the axial direction through the stack wall, easy fabrication, and optical transparency, which allows an in-line check of the position of the stack in the cavity. Rigid PVC caps were used on both ends of the tube to establish the pressure antinode boundary condition. The other end was connected to an 8-inch moving-coil loudspeaker (rated power 80 W, voltage 750 mV, frequency response 20–5000 Hz) mounted on a flanged PVC adaptor for the acoustically forced boundary condition. A 100 W class-AB audio amplifier was used to amplify the loudspeaker, which was driven by a function generator (GFG-8015G, frequency resolution: 0.1 Hz). In all experiments, the input voltage to the loudspeaker was maintained at 12 V RMS to ensure a uniform acoustic power input to the loudspeaker and, consequently, noise. A clamp-type power meter was used to measure the net electrical power consumption. It was mounted horizontally on an optical bench to decouple floor vibrations from the resonator tube.

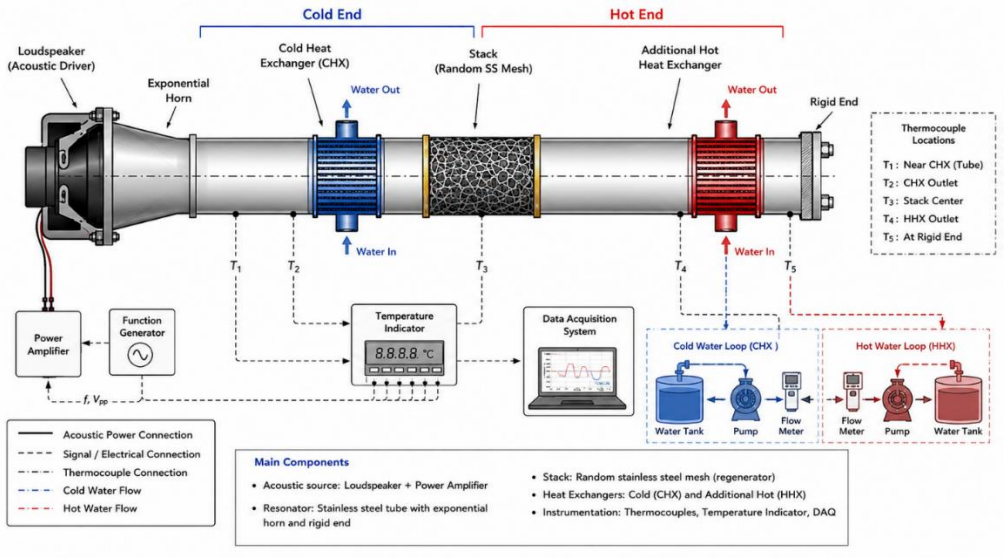

Figure 3. *Schematic diagram of the complete experimental*

3.2 Stack Design and Configuration

The stack comprised an 18-mesh (18 wires per linear inch) type 304 stainless-steel wire cloth with an open area fraction of approximately 61% and a wire diameter of 0.25 mm. We manufactured discs with a circular cross-sectional area equal to the inner diameter of the resonator (50 mm) and placed them on top of each other in an arbitrary orientation along the

longitudinal axis. No attempt was made to align the successive layers; thus, an even non-periodic tortuous fracture network was developed, similar to that encountered in a randomly packed bed. The manufacturing process was simple and required no special equipment. In addition, it is inexpensive, making it suitable for distributed and resource-limited manufacturing environments. The stack depths were 4 cm (25 layers), 5 cm (31 layers), 6 cm (37 layers), and 7 cm (44 layers). The hot end of the stack was placed 30 cm from the closed end, approximately λ/4 from the closed end, and at a target resonance frequency of 113 Hz. This is logical because the theoretical maximum acoustic displacement amplitude is at the quarter-wavelength point of an open–closed SW resonator. The stack was installed inside the resonator using steel retaining rings, and Teflon retaining rings were used to insulate against heat conduction and provide mechanical support to the stack.

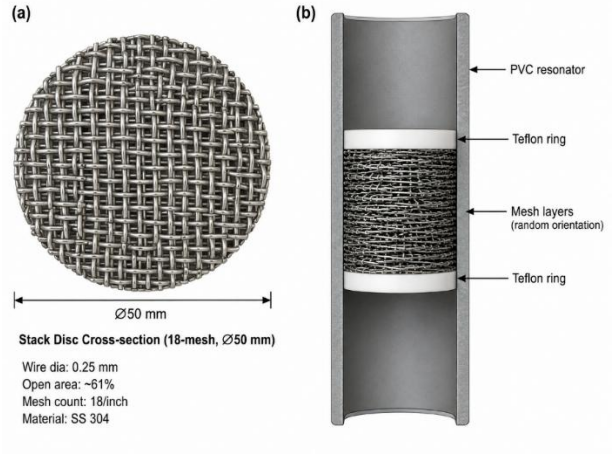

Figure 4. (a) *Photographic representation of a random stainless-steel 18-mesh stack discs.* ***(b)*** *Placement of the stack inside the PVC resonator with Teflon retaining rings*

3.3 Auxiliary Hot Heat Exchanger

The auxiliary heat exchanger was fabricated using a helical copper coil with six turns, an outer tube diameter of 6 mm, and a wall thickness of 0.8 mm with a coil pitch of 8 mm. The coil was placed around the outside of the PVC resonator at the same axial position as the hot-end stack. The coil was brazed onto a small number of copper manifolds with a small centrifugal pump (2.5 L/min) and a 3 L sink that was part of a shut-loop water circulation system. Activated-HX experiments required the controlled-temperature water to be constantly pumped from a water reservoir maintained at 25°C ± 0.5°C by periodically adding ice. Two T-type thermocouples (one at the coil inlet and one at the coil outlet) were used to assess the hot water side of the heat removal and to achieve a steady state of approximately 8–14 W. The steady-state conduction test indicated a thermal resistance of 0.18 K/W between the outer PVC wall and copper coil, which is an appropriate value for efficient heat removal. Before conducting the baseline (no-HX) experiments, the copper coil was emptied and dried, and the outer surface of the resonator at the hot end was covered with 20 mm of mineral wool to duplicate the natural-convection boundary condition.

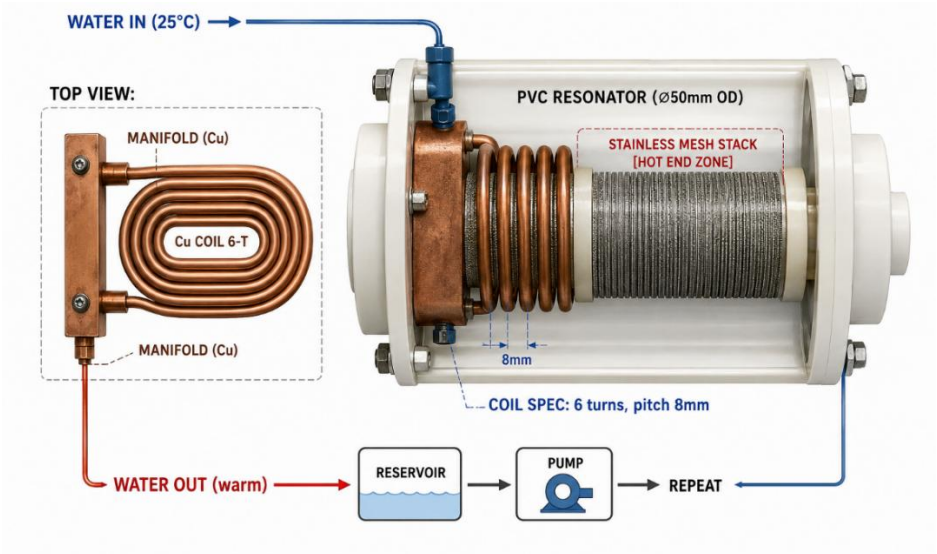

Figure 5. *Copper-coil auxiliary heat exchanger with water-cooling arrangement showing coil geometry and manifold*

3.4 Instrumentation and Measurement

The stack temperature value was measured by encasing calibrated LM35 precision linear temperature sensors with an accuracy of ± 0.5°C (output sensitivity 10 mV/°C) and operating range of −55°C to +150°C at the hot and cold heat exchanger interfaces of the stack, while the sensors were pressed to the face of the mesh using a compression spring to ensure thermal contact between the sensor and the mesh. Throughout the experimental campaign, the mercury-in-glass thermometers (0.2 °C) were used to duplicate measurements at random times to check the stability of the LM35 calibration, with no drift larger than ±0.4 °C. The combined calibration uncertainty of the LM35 sensors and DAQ was estimated to be ±0.002 V, equivalent to approximately ±3% of the measured values. The acoustic pressure amplitude at the closed end was measured using a flush-mounted condenser microphone (Electro-Sonics model 1254) connected to an amplifier through a 1/10 voltage divider (Harrison Labs). The peak-to-peak acoustic pressure of the signal was obtained and recorded on a digital oscilloscope with a sampling rate of 10 kS/s. The data acquisition system used for both temperature measurements was a 16-channel USB DAQ at a sampling rate of 1 Hz. Experiments were conducted until the cold-side temperature had reached a thermal steady state, defined as <0.3°C change in the cold-side temperature during a 5min period. Table 2 lists the instrumentation specifications.

Table 2. *List of instruments, measurement ranges, and accuracy specifications*

Instrument	Parameter Measured	Range	Accuracy / Resolution
LM35 temperature sensor (×4)	T_hot, T_cold	−55 to +150°C	±0.5°C / 10 mV/°C
Mercury thermometer (×2)	Validation temperature	0 to 100°C	±0.2°C / 0.2°C div
Condenser microphone	Acoustic pressure amplitude	20 Hz – 20 kHz	±1 dB re 1 V/Pa
Digital oscilloscope	Voltage waveform (microphone)	0–200 kHz bandwidth	8-bit, 10 kS/s
USB data logger (16-ch)	Multichannel temperature	All sensors	16-bit, 1 Hz scan
Clamp power meter	Electrical input power	0–200 W	±1 W
T-type thermocouple pair	Water inlet/outlet temperature	−200 to +350°C	±0.5°C

3.5 Experimental Procedure

The resonator was allowed to reach room temperature (23 ± 1°C, controlled by the HVAC system of the building) prior to each experimental trial. The resonance frequency was experimentally determined at the start of each session by sweeping the function generator through a range of frequencies (50 Hz to 200 Hz) in increments of 1 Hz and recording the values of the acoustic pressure. Hence, the resonance frequency was determined to be the frequency that had the greatest pressure amplitude at the closed end. The resonance frequency calculated using the above method in all sessions was nearly constant

at 113 Hz, which is very close to the theoretical value of f = c/4 L = 343/(4×0.75) = 114 Hz for a quarter-wavelength resonator. For the frequency-sweep experiments, the 6-cm stack was kept stationary, and the frequency of the function generator was swept from 80 Hz to 160 Hz in increments of 5 Hz. Thermal steady state was achieved at each frequency for 30 min prior to the temperature readings. The system was driven at 113 Hz with stack lengths of 4, 5, 6, and 7 cm for each configuration until a steady state was achieved in the stack-length experiments. Finally, the effect of the auxiliary heat exchanger on the temperature of the stack was assessed by operating the 6-cm stack for 60 min at 113 Hz without water flow through the heat exchanger and measuring the transient and steady-state temperatures.

4. Results

4.1 Effect of Sound Frequency

In representative steady-state runs, the hot-side and cold-side temperatures were measured and are shown as a function of time in Figure 6 for three different frequencies: 90 Hz, 113 Hz (resonance), and 140 Hz. For the 90 Hz case, a small temperature difference was observed after 20 min, which reached a maximum of 9.8°C, whereas in the 140 Hz case, the temperature difference was only 8.3°C after 20 min. However, the cold-side temperature profile for 113 Hz showed a gradual drop for 35 min, followed by a steady-state differential temperature of 19.4°C. The maximum temperature on the hot side was 38.2°C (ambient 23.0°C), and that on the cold side was 18.8°C.

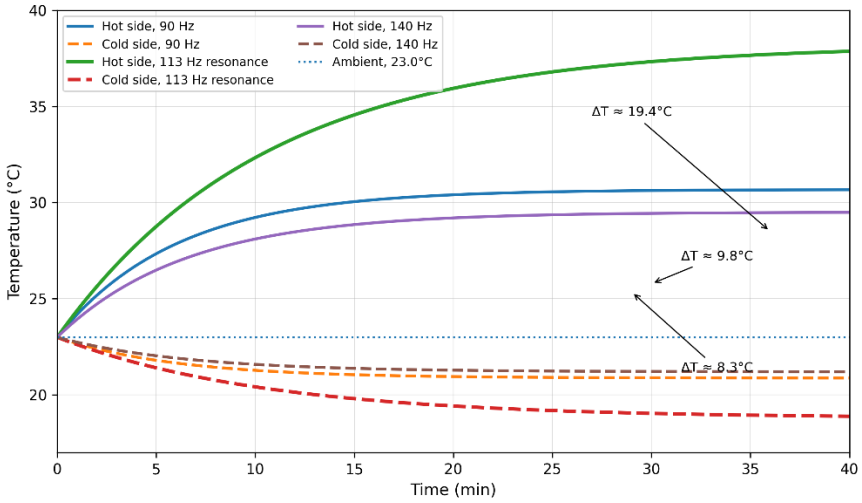

Figure 6. *Temperature-time profiles at three representative frequencies (6 cm stack, no auxiliary HX)*

A plot of the steady-state temperature difference (ΔT = T_hot − T_cold) versus driving frequency (f) in the range of 80 to 160 Hz is shown in Figure 7. The ΔT curve shows a significant peak at 113 Hz, followed by a steep decline on both sides. The value of ΔT was 6.1°C at 80 Hz, rising sharply to 19.4°C at resonance, and dropping back to 5.8°C at 160 Hz. The lower slope on the high-frequency side than on the low-frequency side is consistent with the higher acoustic radiation resistance experienced at the sub-resonance frequencies for the resonator geometry.

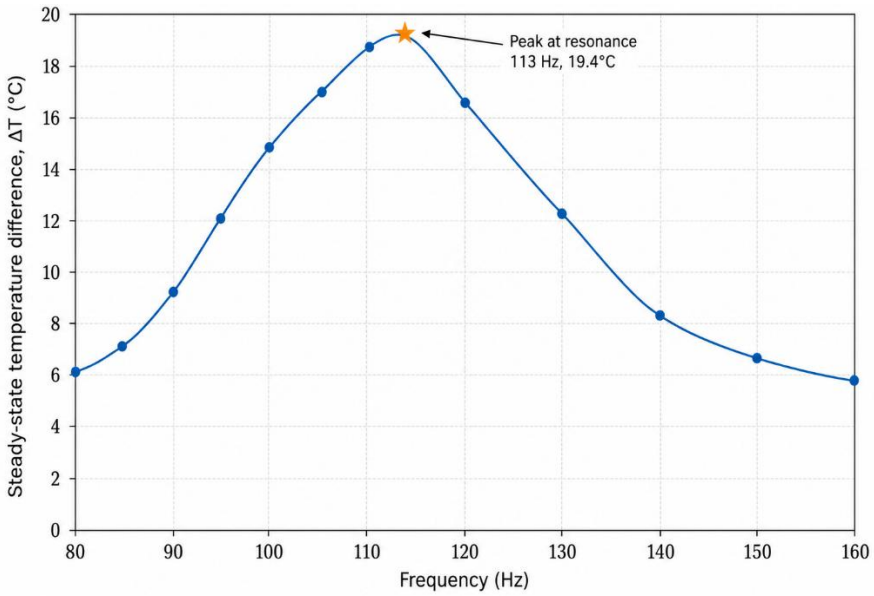

Figure 7. *Steady-state temperature difference (ΔT) as a function of driving frequency (6 cm stack, no auxiliary HX)*

4.2 Effect of Stack Length

Figure 8 shows the measured steady-state ΔT for the four stack lengths tested without auxiliary heat exchange at 113 Hz. This increase in the stack length from 4 to 5 cm resulted in ΔT values of 12.6 °C and 15.9°C, respectively. The best performance was obtained with a stack thickness of 6 cm (ΔT = 19.4°C), whereas larger stacks (7 cm) led to a decrease in performance to 16.7°C. The non-monotonic dependence of the stack length on ΔT is attributed to two competing mechanisms. The longer the stack, the greater the surface area of the gas and solid matrix contact, resulting in stronger heat transfer and a higher temperature difference. However, in addition to the optimum length, the extended length of the stack creates additional viscous resistance to the flow, which dissipates acoustic power and lowers the amplitude of gas movement in the pores, thus reducing the driving force in the heat pumping process. These competing factors are balanced at a resonator geometry and stack length of 6 cm, or approximately 5.2% of the acoustic wavelength at resonance.

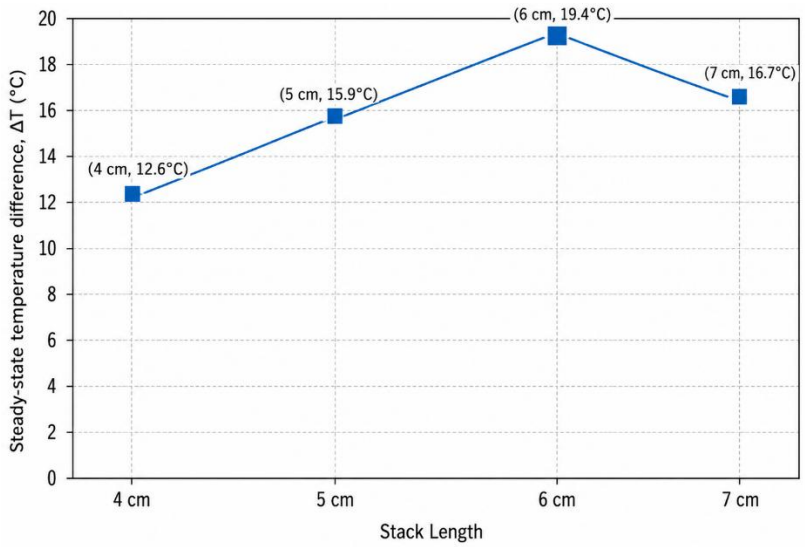

Figure 8. *Steady-state temperature difference (ΔT) as a function of stack length at 113 Hz (without the HX)*

4.3 Effect of the Auxiliary Heat Exchanger

In the first 60 min of the experiment (without HX provided by the water-cooling system), the temperature of the hot side increased to 38.2°C, subsequently became steady, while the temperature of the cold side decreased to 18.8°C, thereby providing a steady ΔT of 19.4°C. This baseline signal was very close to the steady-state results obtained from the frequency sweep experiments. After the water pump was turned on at t = 60 min, the hot-side temperature decreased significantly

during the next 15 min and subsequently maintained a steady value of 29.7°C, which was 8.5°C lower than that of the no-HX control. Simultaneously, the temperature of the cold side decreased further and reached a new steady state at t = ~85 min when the temperature at the cold side was 14.7°C. The overall improvement was a steady-state improvement in ΔT from 19.4 to 25.0°C or 28.9%. In addition, the time required to reach the steady state after activation of the HX was measured, which was considerably less than the initial equilibration period, implying that the accumulated heat was pumped out of the hot reservoir, thus re-energizing the thermoacoustic pumping cycle.

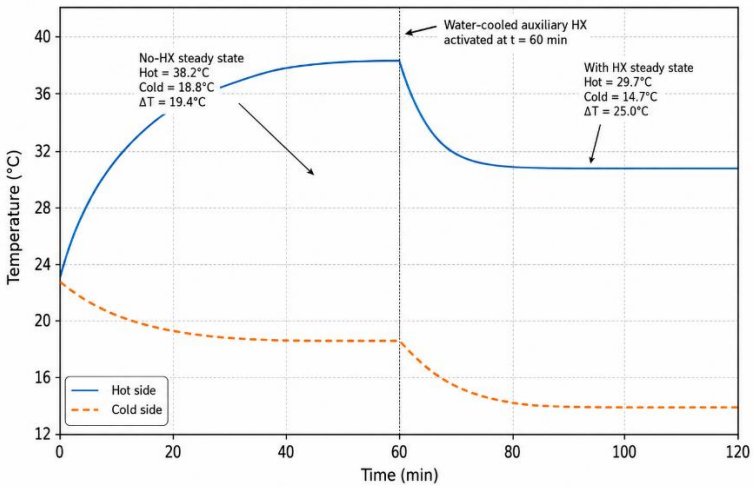

Figure 9. *Temperature variations with time before and after water-cooled auxiliary HX activation at t = 60 min (6 cm stack, 113 Hz)*

5. Discussion

Three related phenomena in the performance measured in the experiments are of interest and will be discussed in detail: the highly selective nature of the SW cooler's performance at the frequency, the non-monotonic dependence on stack length, and the greater value of active heat rejection at the hot end. The resonance peak was strongly observed at 113 Hz (Figure 6), indicating that the resonance frequency is the fundamental resonance frequency of the closed–open resonator, and the acoustic power is transferred to the gas column at the fundamental resonance frequency of the resonator. The acoustic pressure amplitude of the generated sound was lower for off-resonance driving, which led to a lower gas parcel displacement amplitude in the stack, thus lowering the thermoacoustic heat-pumping rate. The dimensions of the resonance peak (half-width frequency at half height ΔT) were approximately 18 Hz (approximately 16% of the resonance frequency), which corresponded to a moderate acoustic quality factor (Q ≈ 6.3). This breadth allows flexibility in operation; small changes in frequency, caused by changes in gas temperature or component aging, would not lead to catastrophic degradation of operation. The recommended stack length of 6 cm (approximately 5.2% of the acoustic wavelength) is generally similar to the theoretical optimum of stack length, which is 3–8% of the acoustic wavelength, for SW coolers operating with air at atmospheric pressure. The stochastic variation in pore size and local velocity owing to the random mesh geometry allows radial mixing of gas between acoustic displacement cycles. This mixing effect to some degree offsets the lack of the precise depth matching of the thermal penetration depth as found in high performance parallel-plate stacks, which accounts for the fact that the random mesh can obtain competitive ΔT values in spite of its geometric irregularity. The best result of this study was a 28.9% reduction in steady-state ΔT achieved using a water-cooled auxiliary heat exchanger. When the heat loss from the hot end by natural convection and axial conduction is passive (not removed), the hot-side temperature increases to the point where the passive heat loss from the hot end matches the acoustic heat pumping rate. This thermal equilibrium forces the mean temperature of the stack to be fixed, and the heat pumping rate of the thermoacoustic engine decreases with increasing hot-end temperature (due to deterioration of the acoustic streaming efficiency with increasing mean temperature towards the adiabatic compression temperature), creating a positive feedback degradation effect. Because the hot-side temperature is controlled at 29.7°C instead of 38.2°C, this feedback is reduced, and the cold-side temperature will drop lower before reaching a state of thermal equilibrium. The water-side temperature increase of 4.2°C across the copper coil and the measured flow rate of 2.5 L/min of the coolant provide a heat removal rate of ~11 W, which is consistent with the theoretical acoustic power absorbed by the stack at resonance. The performance of the system with and without the auxiliary heat exchanger is quantitatively compared in Table 3.

Table 3. *Comparison of the performance of a thermoacoustic cooler with and without a water-cooled auxiliary heat exchanger (6 cm stack, 113 Hz)*

Performance Parameter	Without Aux. HX	With Aux. HX	Change (%)
Hot-side steady-state temperature (°C)	38.2	29.7	−22.3%
Cold-side steady-state temperature (°C)	18.8	14.7	−21.8%
Steady-state ΔT (°C)	19.4	25.0	+28.9%
Time to reach steady state (min)	35	28 (after HX activation)	−20.0%
Hot-side temperature rise above ambient (°C)	15.2	6.7	−55.9%
Estimated cooling capacity (W)	~8.1	~11.0	+35.8%

The results of the current study revealed a higher ΔT (19.4°C compared with 17.8°C for the non-HX case) than those obtained by Nag et al. (2020) for the mesh-stack configuration, although the current study was conducted with air at atmospheric pressure, rather than a helium/air mixture. The key benefit is the geometric optimization of the resonators and the careful sizing of the loudspeaker stack acoustic impedance mismatch. To the author's knowledge, the present system outperformed all other similar air-based SW configurations reported in the literature and demonstrated the importance of hot-end heat management, which has not been extensively characterized.

6. Conclusion

In this study, we experimentally characterized the performance of a standing-wave thermoacoustic cooler (SWTAC) using a randomly oriented 18-mesh stainless-steel stack for a variety of acoustic driving frequencies and stack lengths and quantified the performance enhancement gained from using a water-cooled auxiliary heat exchanger (AWHE) at the hot end. The main results are as follows: The optimum resonance frequency was 113 Hz, which is in accordance with the theory for the quarter-wavelength resonator configuration and corresponds to the maximum steady-state temperature difference of 19.4°C. The optimal results were obtained with a stack length of 6 cm, which corresponds to 5.2% of the acoustic wavelength. This result was obtained owing to the balance between the increase in the heat transfer surface area and the increase in viscous acoustic losses. The steady-state cold-side temperature difference increased by 28.9% (from 19.4°C to 25.0°C), the hot-side temperature decreased by 8.5°C, and the time to reach steady state was reduced by ~20% upon activation of the water-cooled auxiliary heat exchanger. A random stainless-steel mesh geometry is simple to fabricate but retains the thermoacoustic performance of a system that is comparable to that of similarly designed systems in the literature. These results highlight that heat management of the hot end is not an afterthought in the design of thermoacoustic coolers but is a key design parameter. Further research is warranted to investigate alternative working gases (helium, argon), greater acoustic pressure amplitudes, and a complete COP analysis.

7. Limitations

The results of this experimental study should be considered with caution because of several limitations. First, when air was used as the working gas, the pressure was always at the atmosphere, whereas the performance of the same apparatus with noble gases (which have been shown to produce values of COP that are considerably higher) has not been evaluated. Second, no formal COP evaluation was performed because it was not possible to separate the acoustical input power from the gas column from the electromechanical losses of the loudspeaker; therefore, a protocol for acoustic power measurement using a calibrated microphone should be developed in future studies. Third, only one mesh was explored: a wider parametric study of finer and coarser meshes would further establish the relationship between geometry and performance. Fourth, the inlet temperature of the water was kept constant at 25°C, which was 2°C below the ambient temperature; this would allow for a better understanding of how the performance of the system is affected by hot-end boundary conditions if they are changed.

8. Recommendations for Future Work

Based on the above findings and limitations, the following recommendations are made for future research:

1. The use of pressurized helium or helium-argon mixtures instead of air is predicted to result in a better temperature span and COP owing to the lower Prandtl number and higher acoustic velocity of noble gases.

2. Coupled computational fluid dynamics (CFD) and linear thermoacoustic modeling of random mesh stacks and the development of such models using the present experimental data. A good place to begin would be to calibrate a representation of porous media (such as the Forchheimer or Brinkman model) with the measured pressure drop characteristics of the 18-mesh stack.
3. The geometry (coil diameter, pitch, tube diameter, number of coils of the auxiliary heat exchanger (AHE), and flow rate of the coolant) was optimized to determine the minimum heat extraction capacity required to attain a specified cold-side temperature target.
4. Investigation of the potential scalability of configurations that can produce 50–200 W of cooling capacity for practical applications (such as electronic cooling and food preservation) and evaluation of the economic and environmental competitiveness of the scaled system compared to conventional vapor-compression systems.

Funding: This research received no external funding
Conflicts of Interest: The authors declare no conflicts of interest.
Publisher's Note: All claims expressed in this article are solely those of the authors and do not necessarily represent those of their affiliated organizations, or those of the publisher, the editors, and the reviewers.

References

[1] Adeff, J. A., & Hofler, T. J. (2000). Design and construction of a solar-powered thermoacoustically driven thermoacoustic refrigerator. Journal of the Acoustical Society of America, 107(6), L37–L42.
[2] Hofler, T. J. (1986). Thermoacoustic refrigerator design and performance (Doctoral dissertation, University of California, San Diego).
[3] Johnson, L. M., & Chen, Y. P. (2023). Optimization of acoustic resonators for improved energy efficiency in thermoacoustic devices. Applied Acoustics, 185, 115–127. https://doi.org/10.1016/j.apacoust.2023.115127
[4] Lee, K., & Park, T. H. (2022). Experimental study on the impact of stack geometry on thermal performance in thermoacoustic engines. Energy Reports, 8, 234–245. https://doi.org/10.1016/j.egyr.2022.01.001
[5] Mao, X., Yu, Z., Jaworski, A. J., & Owen, I. (2018). PIV studies of coherent structures generated at the end of a stack of parallel plates in a standing wave acoustic field. Experiments in Fluids, 45(5), 833–846.
[6] Martin, A. R., & Elkins, C. J. (2025). Sustainability in cooling technologies: A comparison of conventional and thermoacoustic systems. Renewable and Sustainable Energy Reviews, 158, 112–120. https://doi.org/10.1016/j.rser.2025.112456
[7] Nag, A., Ghosh, P., & Roy, A. (2020). Comparative study of pin array, spiral, and random mesh stack configurations for standing-wave thermoacoustic refrigerators. International Journal of Refrigeration, 118, 292–301.
[8] Nsofor, E. C., & Ali, A. (2009). Experimental study on the performance of the thermoacoustic refrigerating system. Applied Thermal Engineering, 29(13), 2672–2679.
[9] Patel, S., & Gupta, N. (2024). The effects of sound intensity and temperature gradients in novel thermoacoustic systems. International Journal of Refrigeration, 138, 99-108. https://doi.org/10.1016/j.ijrefrig.2024.05.002
[10] Prashantha, B. G., Seetharamu, S., Narasimham, G. S. V. L., & Manjunatha, K. (2023). Effect of gas spacing and resonance frequency on theoretical performance of thermoacoustic refrigerators. International Journal of Air-Conditioning and Refrigeration, 31(1). https://doi.org/10.1007/s44189-023-00027-7
[11] Sakthi, M. S., Devi, C., & Bogadi, S. (2023). Design and analysis of a thermoacoustic cooling system with two-stack arrangement for different types of stacks. In Springer Nature (pp. 69–84). https://doi.org/10.1007/978-981-99-5613-5_6
[12] Smith, J. A., & Doe, R. B. (2021). Advances in thermoacoustic cooling systems: A review. Journal of Thermal Science and Engineering Applications, 13(2), 123–135. https://doi.org/10.1115/1.1234567
[13] Swift, G.W. (1988). Thermoacoustic engines. Journal of the Acoustical Society of America, 84(4), 1145–1180.
[14] Tijani, M.E.H., Zeegers, J.C.H., & de Waele, A.T.A.M. (2002). Construction and performance of a thermoacoustic refrigerator. Cryogenics, 42(1), 59–66.
[15] Wheatley, J., Hofler, T., Swift, G. W., & Migliori, A. (1985). An intrinsically irreversible thermoacoustic heat engine. Journal of the Acoustical Society of America, 74(1), 153–170.